# MASONRY DAMS – ANALYSIS OF THE HISTORICAL PROFILES OF SAZILLY, DELOCRE AND RANKINE

E.M. Bretas, J.V. Lemos, P.B. Lourenço

Eduardo M. Bretas, email: eduardombretas@gmail.com, Universidade do Minho, Departamento de Engenharia Civil, P-4800-058 Guimarães, Portugal, Tel: +351 218443000, Fax: +351 218443011

José V. Lemos, email: vlemos@lnec.pt, Laboratório Nacional de Engenharia Civil, Departamento de Barragens de Betão, Av. do Brasil, 101, 1700-066 Lisboa, Portugal, Tel: +351 218443000, FAX: +351 218443011

Paulo B. Lourenço, email: pbl@civil.uminho.pt, Universidade do Minho, Departamento de Engenharia Civil, P-4800-058 Guimarães, Portugal, Tel: +351 253510200, Fax: +351 253510217

## Abstract

The significant advances in masonry dam design that took place in the second half of the 19th century are analyzed and discussed within the context of the historical development of dam construction. Particular reference is made to the gravity dam profiles proposed by Sazilly, Delocre and Rankine, who pioneered the application of engineering concepts to dam design, basing the dam profile on the allowable stresses for the conditions of empty and full reservoir. These historical profiles are analyzed taking into consideration the present safety assessment procedures, by means of a numerical application developed for this purpose, based on limit analysis equilibrium methods, which considers the sliding failure mechanisms, the most critical for these structures. The study underlines the key role of uplift pressures, which was only addressed by Lévy after the accident of Bouzey dam, and provides a critical

understanding of the original design concepts, which is essential for the rehabilitation of these historical structures.

**Keywords**

Masonry dam; gravity dam; uplift pressure; failure mechanism; safety assessment

## 1. Introduction

During the second half of the 19th century, within the framework of a more comprehensive social and cultural movement, the first scientific works about dam design were published. These works adopted a novel approach as they admitted, for the first time, that this activity had technical and scientific nature, besides the traditional empirical character (Smith 1971). Special reference must be made to the theoretical profiles proposed by Sazilly (1853), Delocre (1866) and Rankine (1881, first publication in 1872), because these directly influenced the construction of a large number of dams, many of which are still in operation. The fact that the uplift effect was still unknown at the time, and therefore was disregarded in the design, is the main weakness of these structures, which has justified the need for various rehabilitation and strengthening interventions.

In the rehabilitation of existing structures it is valuable to know the assumptions of the original designs, as safety becomes easier and more reliable to assess. In the present work, the fundamental concepts behind the historical profiles of dams are analyzed, within the context of the developments in scientific and engineering knowledge. A key failure mechanism in gravity dams, either built of masonry or concrete, involves sliding on horizontal planes, which may include joints in the foundation rock mass, the dam foundation surface, masonry joints or concrete lift joints. At present, the rules to perform this global stability analysis, including the water pressure diagram to be assumed along the failure surface, are essentially common to the main design codes (e.g. Ebeling et al. 2000; Ruggeri 2004). These procedures were applied in

the stability analysis of the three historical profiles referred above, with the aim of evaluating the most likely failure scenarios and characterizing the global behavior of these structures. A numerical application was developed for this purpose, based on limit analysis equilibrium methods, which are typically employed in this type of assessment (e.g. Leclerc, Léger, and Tinawi 2003).

A brief historical background is presented here, covering the development of dam construction, especially, of the masonry gravity dams built in Europe. Reference is also made to the transition from straight to arch dams, and from masonry to concrete dams, as well as to the evolution in analysis methods, integrating them into the design and construction of the most important masonry and concrete dams of the period under analysis.

## 2. Historical background

### *Roman dams*

The need to store water, in particular in dry areas, was probably the main reason for the construction of the first dams, which consisted of earth structures built in 3000 B.C., in Jawa, present Jordan, the highest being 4m high and having a length of 80m (Figure 1a). These are considered to be the oldest known dams. Moreover, from among the oldest ones, the tallest, known as Sadd-el-Kafara (Figure 1b) and located close to Cairo, was built by the Egyptians in 2600 B.C., in accordance with the same construction procedure, and was 14m high and 113m long (Jackson 1997). In Europe, particularly in the Iberian Peninsula, the oldest dams remaining are Roman. The management skills of Romans, associated with the technique inherited from Egyptians, (Quintela, Cardoso, and Mascarenhas 1987) left relevant examples of 20 large dams built (Laá 1993), out of about 80 documented dams (Schnitter 1994). An important contribution by the Romans was the use of hydraulic lime, apart from traditional materials, such as earth and rock.

The most common structural typologies were gravity dams with trapezoidal cross-sections, buttress reinforced gravity dams or dams integrating multiple solutions, such as masonry walls reinforced with embankment slopes.

It is assumed that the oldest Roman dam in the Iberian peninsula, probably built in the 2nd century, is the Alcantarilla dam (Figure 1c) (H=17m, L=557m)[1], located at 20km from Toledo. The dam presented a cross-section integrating two external stone masonry walls and its interior was filled by backfill material. In the downstream side, a slope was created to withstand the hydrostatic pressure (Jansen 1980). The dam is presently in ruins. By observation of the relative position of the ruins, located upstream of the original construction site, it is possible to conclude that the failure was likely to have occurred due to the downstream slope, probably during a sudden emptying of the reservoir (Jansen 1980).

Also around the 2nd century, the Proserpina dam was built (Figure 1d) (H=22m, L=426m), close to Mérida. The characteristics are similar to the ones in the Alcantarilla dam, except for the fact that the latter presents a group of nine buttresses, close to the upstream face, which support the thrust of the downstream slope, in case the reservoir needs to be emptied. The dam maintains its original function, which is to supply water to the city of Mérida (Jansen 1980).

Cornalbo dam (Figure 1e) (H=24m, L=220m), which was probably built in the same period as the Proserpina one. In terms of design, it is similar to a fill dam, with a masonry core and a slope in each face. The slope of the upstream face has the particularity of consisting of 3 masonry walls, parallel to the dam, and other transversal ones, forming cells filled by backfill and masonry cover. This dam is still in operation (Laá 1993). Cornalbo dam has been considered the tallest Roman dam located outside the Italian territory (Schnitter 1994), but

[1] Where appropriate, the maximum height (H) and the crest length (L) are indicated next to the name of the dam.

other authors refer to Almonacid de la Cuba Dam as the tallest Roman dam, with 34m (Parra et al. 1995).

In Portugal, Olisipo dam (H=8m, L=64m) (Figure 1f) is the tallest known Roman buttress dam[2]. That dam was built over Carenque river, located in Belas, probably in the 3rd century and was the starting point of an aqueduct to Olisipo (Lisbon). It had a storage volume of $110x10^3m^3$ and occupied a floodable area of 4.7ha, for a reservoir with a perimeter of 1.9km. The dam ceased operation at the time of construction of *Águas Livres Aqueduct*, in the 17th century, when it was partially destroyed close to the right bank, where a structure was built with a shaft to inspect the channel of the new structure (Almeida 1969).

An arch dam, 40m high and built according to Nero's decision in the 1st century for recreational purposes, together with other two dams forming part of Vila Subiaco close to the Aniene river, must also be mentioned. These dams are thought to be the only ones built by Romans in their own territory. They were used for water supply to Rome, through an aqueduct with construction initiated by Caligula (38 A.C.) and was afterwards completed by Claudius (50 A.C.) (Smith 1971).

***Developments until the 19th Century***

After the end of the Roman empire, the structural design and the construction methods used in the dams, almost invariably followed the models inherited from the Romans, particularly in the south of Europe, which were mostly masonry dams. On the contrary, in the north of Europe, fill dams were usually built.

Taking Spain as an example[3], until the 15th century, during and after the Arab period, the only relevant aspect was the construction of a large number of weirs. These dams, of small size and having an overflow cross-section to raise the level of a river or stream, were used for

[2] In Spain, Esparragalejo and Araya buttress dams respectively are 5.5m and 4.0m high (Laá 1993). Esparragalejo dam is an arch dam, which is buttress reinforced.

[3] Spain is probably the country in which the highest number of masonry dams was built throughout history, making a landmark in the development of dams (Vogel 1981). Presently, it has 158 large masonry dams in operation.

temporarily retaining water, just for the time necessary to ensure the partial diversion of the water or for irrigation purposes. These downstream sections also ensured energy dissipation in case of flood (Schnitter 1994). As the 17th century was a period of economic decline, the main dams were built from private initiative. Three arch dams must be stressed, namely, Tibi dam (Figure 1g) (H=46m, L=65m) with a radius of 97m, Elche dam (Figure 1h) (H=23m, L=95m) with a radius of 62m and Relleu dam (Figure 1i) (H=29m, H=34m) with a radius of 60m. In the 18th and 19th centuries, the economic development and a favorable legal framework for the management of water resources led to the construction of new dams. Nevertheless, the prevailing structural scheme was based on trapezoidal cross-sections with a large volume, following the Roman tradition, despite the tendency for reduction of cross-sections (Laá 1993).

In other European regions, water was also increasingly used, particularly for producing mechanical energy for mining, namely in the exploitation and treatment of ore. Apart from this purpose, other economic activities justified the construction of dams, namely: fishing, irrigation for farming, irrigation for gardening and for fountains, water supplying, and canals for boat transportation of goods. Mention must be made also to the fact that water was not retained close to the water line, but was rather diverted through canals to more adequate sites. This was also intended to reduce the flood consequences in case of mechanical energy production (Schnitter 1994).

***Developments in the second half of the 19th century***

In 1853, J. Augustin Tortene de Sazilly published in *Annales des Ponts et Chassées* the work *"Note sur un type de profil d'égale résistance proposé pour les murs de réservoirs d'eau"*[4], which was considered to be the first scientific document[5] in this field. Many other works had

[4] "Note on a section of equal resistance proposed for the walls of water reservoirs".
[5] Reference must also be made to Simon Stevin's work ("*De Beghunselem des Waterwichts*"), published in 1586, about the hydrostatic pressure on a wall and to Bernard Forest de Belidor's work ("*Architecture Hydraulique"*),

already been published, but these were no more than records of the construction solutions used or devised at the time, without mentioning any scientific design criteria (Smith 1971).

According to Sazilly, the cross-section of the dam should be designed so as to avoid the failure by excessive compressive stress and by sliding. Both scenarios should be observed at the contact between the dam and foundation, but also along the body of the dam. Also according to Sazilly, the sliding scenario had never been observed in any previous failure, so design of the cross-section should just take into account only the first criterion, while the sliding scenario should be verified afterwards. In accordance with Sazilly's reference, the proposed stress analysis was based on M. Méry's work[6], about the stability of arches, which was disclosed by M. Bélanger in the Cours de Mécanique Appliquée (Course of Applied Mechanics) delivered at L'École Nationale des Ponts et Chaussées (National School of Bridges and Roads), France.

By characterizing the two extreme load scenarios, dam with empty and with full reservoir, Sazilly established a limit value for the maximum vertical stresses installed on the upstream and downstream faces, in any possible horizontal plane of the body of the dam and at its base. Since the limit stress is equal for both cases, it justifies the adopted designation of "profile of equal resistance" (Wegmann 1899)[7]. Sazilly formulated the differential equations that allow to solve the problem in mathematical terms, which he denoted[8] as "theoretical profile", but he was unable to perform their integration. Thus, he proposed a "practical profile", achieved by the discretization of the body of the dam into horizontal slices, which led to the creation of a stepped profile.

published in 1750, about the resistance to collapse of a wall with a rectangular cross-section under the action of water on one of its faces.

[6] In 1826, Louis Navier published his first studies about the analysis of stresses and the modulus of elasticity.

[7] Author and date of publication of the book entitled "The design and construction of dams", which addresses design criteria and presents case studies.

[8] The terms "theoretical section" and "practical section" are included in Sazilly's studies and are adopted by other authors in subsequent documents.

Figure 2 shows this profile, in the version developed by Wegmann (1899) based on Sazilly's formulation, for a height of 50m and a limit stress of 6kgf/cm² (0.59MPa). The section included in the original Sazilly's work has a height of just 30m. He also envisaged the possibility of approximating the curve using rectilinear sections, but he considered that the intersection points would be weak points, as well as possible points of accumulation of dirt and vegetation and would introduce additional construction complexity (Sazilly 1853).

The evaluation of the sliding resistance should be done after the definition of the practical profile. Whenever sliding was possible in the body of the dam, the profile could be altered, in particular by increasing the crest thickness. If sliding occurred at the base, a downstream wall could be adopted to counteract that movement.

The first project to be developed according to the principles proposed by Sazilly was Furens dam (H=50m, L=200m). In 1858, A. Graeff and F. Emile Delocre initiated the process of selection of the site and subsequently the design of the dam that would be, for about 10 years, the largest in the world. Located in the vicinity of Rochetaillée, close to Saint Etienne, in France, the construction of the dam began in 1860 and the first filling took place in 1866 (Hager and Gisonni 2007).

In the stage of design, Delocre initially used the "practical section" proposed by Sazilly, changing the configuration of the faces to a polygonal profile (Figure 3). When comparing the two hypotheses, he concluded that there were no significant differences in the safety factors and the solution found allowed to save in material. Only in 1866, after completion of the dam, Delocre disclosed his work in *Annales des Ponts et Chassées*, titled "*Mémoire sur la forme du profil à adopter pour les grands barrages en maçonnerie de réservoir*"[9]. Indeed, Furens dam

[9] "Report on the profile shape to be adopted for large masonry reservoir dams"

is an important landmark in dam design, particularly in France[10], where 47 gravity masonry dams were built before 1866.

Another fundamental contribution was given by S. Rankine in 1872, with the publication of an article in *The Engineer*, with the title "*Report on the design and construction of masonry dams*". In this article, Rankine confirms the validity of the former works by Sazilly's and Delocre's (Wegmann 1899). The sole difference consists of the use of different limit stress values for extreme load cases. Since the limit stress is a vertical stress, the use of a lower limit stress for the downstream face is proposed, because the larger angle with the vertical leads to a higher principal stress when compared with the upstream face. Since no mathematical formulation was used for defining these limits, just by taking into account the observation of existing works, Rankine suggested the limit of 9.8kg/cm² (0.96MPa), for upstream, and 7.6kg/cm² (0.75MPa), for downstream (Rankine 1881).

Rankine introduced the principle, that even though not opposed to the basic principles of Sazilly's method of the "profile of equal strength", is more comprehensive, which is defines the important requirement of avoiding the occurrence of tensile stresses in any point of the dam. This determines that the static resultant in each horizontal section should remain within the central third of the corresponding section[11]. The practical section he proposes is based on the adoption of curved walls with a logarithmic configuration (Figure 4).

Apart from describing the state of the art in dam design, Rankine made also some considerations about the quality of the foundations, in particular requiring the selection of sound or slightly weathered rock masses for the foundations. He also stressed the importance of the construction technique, requiring to fill voids with stones with hydraulic lime acting only as aggregation element and avoiding using lime to fill large voids. In the calculations

[10] In France, there are 56 masonry dams in operation. The oldest one is Saint Ferréol dam, 35m high, built in 1672, with a typology similar to Roman dams, in terms of volume and of the combined use of masonry and earth walls (Royet et al. 1993).

[11] Such criterion also implicitly prevents the failure by an overturning scenario.

presented, the vertical component of the hydrostatic pressure due to the inclination in the upstream face is neglected (Rankine 1881).

None of the works mentioned explicitly considered the existence of uplift water pressures, situation that was probably altered with the accident in Bouzey dam (Figure 1j) (H=23m, L=525m), which collapsed in 1895, as a result of the effect of uplift, having caused 85 victims (Smith 1971). The book "High Masonry Dams" by J.B. McMaster, published in 1876, previous to the accident of Bouzey dam, does not take the uplift in consideration, but the book "Engineering for Masonry Dams" by W.P. Crager, published in 1917, after the accident, considers all relevant loads, uplift included. The accident had a great impact among dam designers, who assumed subsequently that all the necessary criteria for designing safe structures were completely defined (Smith 1971).

As a result of this accident, still in 1895[12], M. Lévy published by the *Académie des Sciences*, an article entitled "*Quelques considérations sur la construction de grands barrages*"[13] (1895), in which he states that the compressive stress on each point of the upstream face must be equal or higher than the water pressure at this point. In fact, apart from the stability problems of the section, cracks may occur by other processes, such as thermal loads, and this new criterion was defined to take this into account. As a result, a triangular uplift diagram, or trapezoidal, depending on the downstream water level, was to be adopted for any horizontal section of the dam, including the plane of contact between the dam and the foundation. The use of the triangular uplift diagram proposed by Lévy has been current practice since then, but, in the presence of a drainage system, the uplift diagram is reduced, assuming a bi-linear configuration, as discussed below.

Before these events, in 1882, the Vyrnwy dam was designed (Figure 1k) (H=40m, L=412m), near Liverpool, in England (Smith 1971). This dam was the first to have a drainage system at

[12] The accident occurred in April 1895 and Lévy's article is dated from August of the same year.
[13] "Some considerations on the construction of large dams".

the foundation, which consisted of 26 drains (Wegmann 1899) with dimensions 0.23x0.30m, connected to vertical shafts and to a horizontal gallery with an outlet in the downstream face (Schnitter 1994). These drains were designed by T. Hawksley and G. Deacon, the latter being responsible for conceiving the system and for supervising the entire work (Davidson 1997).

A reference must be made also to Germany, where gravity dams are mainly associated to O. Intze. In 1891, Intze completed the construction of Eschenbach dam (H=24m, L=412m), designed in accordance with a profile that is known as "Intze" type. The dam consisted of a gravity masonry structure, with small curvature in plant and without vertical joints, with a masonry upstream face under a waterproofing layer. Despite lacking a drainage gallery, the dam had vertical drains[14]. A distinguishing element is a wedge-like slope close to its upstream heel, which is present until mid-height of the dam with the purpose of waterproofing. The beginning of the 20$^{th}$ century in Germany was characterized by a strong economic growth that encouraged the construction of dams, with nine dams inaugurated in between 1913 and 1914. Germany[15] has a total of 41 masonry dams in operation, located in the mountainous regions of North Rhine-Westphalia and of Saxony, which were influenced by Intze (Rissler 1993).

It is noted that Rankine also addressed the issue of the in plan dam shape. Despite assuming a favorable effect of an arched shape, he did not find any theoretical justification for its use. This was possibly one of the main reasons for the Zola dam (Figure 1l) (H=42m, L=66m) having remained almost unknown (Chanson and James 2002). The dam, completed in 1854[16], after the death of its designer (F. Zola), has a cylindrical configuration, with a constant radius, for which it was possible to calculate the stresses based on the formulation developed in 1826 by Louis Navier (Jackson 1997). The dam presents a cross-section with variable thickness,

[14] Intze did not consider the uplift as a load in the design.

[15] Germany is an excellent case study for dam rehabilitation, due to the publication of standard DIN 19702, in the 1980s. This standard provided more severe safety conditions, in particular for masonry dams of the "Intze" type, as initial design did not include the uplift load. This led to various interventions, ranging from the reduction of the operation level and the adjustment of spillways to thorough interventions, such as adding a longitudinal drainage gallery close to the base or the application of pre-stress in the crest (Bettzieche, Deutch, and Heitfuss 2004).

[16] It was, until 1887, the tallest arch dam in the world.

which increases towards the foundation where the hydrostatic pressure is higher (Billington, Jackson, and Melosi 2005). Parramatta dam (H=12.5m, L=80m), in Australia, designed in 1851 by P. Simpson, E. Moriarty and W. Randle, and finished in 1856, was probably built as a result of the studies done by Zola (Chanson and James 2002). Also as a result, the work produced in 1879 by A. Pelletreau, suggested a calculation method based on the concept of constant angle and allowing a variation in the radius with the increase in the cross-section towards the base. This led to the Salmon Creek dam (Figure 1m) (H=51m; L=195m) built in 1915, in Alaska, by Lars Jorgensen (Jackson 1997). Afterwards, the double curvature configuration was proposed, which was the most efficient and the most demanding in terms of design (Chanson and James 2002).

***Developments in the 20$^{th}$ century***

Similarly to other civil engineering fields, the configuration of dams evolved towards more slender and sophisticated cross-sections, led by the need to reduce costs and made possible by the increasing knowledge of structural mechanics and the diffusion of concrete as a building material. Buttress dams were developed, initially with a cross-section of the hollow gravity type, reinforced with buttresses, and subsequently by assuming a clear distinction between the element responsible for retaining water (panel) and the one with a structural function (buttress). The design of arch dams required more advanced methods of stress analysis. In this context, special reference must be made to G. Wisner's and E. Wheeler's contributions, who, by request of the *Reclamation Service*, initiated in 1905 studies to better understand the load distribution on arch dams. For this purpose, these authors devised a set of arches adjusted to the dam under design combined with a central cantilever. Using an iterative process that forces compatibility of displacements of the arches, they determined the load distribution across the various sections. This lead to the conclusion that at higher elevations, the behavior of the arch was decisive, whereas close to the bottom the cantilever effect prevailed. Such

method was employed in the design of Pathfinder dam (Figure 1n) (H=65m, L= 132m), Wyoming, USA, which was completed in 1909. In 1929, C. Howell and A. Jaquith, both from the *Bureau of Reclamation* of Denver, formalized this calculation method using various arches and cantilevers, developed through scattered contributions, as the *Trial-Load Method*. This is in opposition to a model with just one cantilever, which had been current practice until then. The development of the finite element method provided the ideal tool for stress analysis of concrete dams, which were, in fact, one of the most important civil engineering applications of the method in the early 1960's, as described by Clough and Wilson (1999).

Seismic action on dams has been considered, in a first approximation, as a static inertial load. This simplified assumption is still used in the study of the global sliding stability of gravity dams, with the hydrodynamic effect of the reservoir represented by the classical Westergaard (1933) concept of the water added-mass. The analysis of the dynamic structural response of dams, particularly important for arch dams, was only made widely available with the development of the finite element method.

The trend towards more complex forms of concrete dams has been reversed in recent decades, as roller-compacted concrete (RCC) dams became more widespread, reflecting the predominant cost of the construction process over the cost of the materials. Gravity dam design remains therefore a theme of interest in dam engineering.

During the late 19$^{th}$ century and the early 20$^{th}$ century the scientific basis necessary for modern gravity dam design was established. The main actions, such as self weight and hydrostatic pressure, but also uplift, were fairly well studied in this period. Nevertheless, aspects such as foundation strength, long term behavior of materials, permeability or

earthquakes received less attention, eventually clarified with experience and later developments in science and technology.

Global stability analysis remains an indispensable component in the safety evaluation of gravity dams, considering the possibility of various sliding mechanisms, which may take place along the foundation surface or involve rock joints (e.g. Rocha 1978). The accident of the Malpasset arch dam in 1957 stressed the importance of the hydromechanical behavior of rock foundations (Londe 1987). Knowledge on issues such as the effectiveness of the grout curtain and drainage systems progressed with extensive field monitoring (Casagrande 1961). These data provide the means to validate and calibrate numerical models of seepage problems, which were already developed in the early days (Serafim 1968). For stability analysis of gravity dams, the diagram of uplift water pressure along the sliding surface is a decisive factor. In the absence of drainage, a triangular or trapezoidal diagram needs to be considered (Figure 5a). When drains are present, a reduction of the water pressure can be considered at the drain location, leading to a bilinear diagram (Figure 5b). It is a common design assumption to adopt a reduction factor of 2/3 (Leclerc, Léger, and Tinawi 2003). However, the possible development of upstream cracking may allow the full reservoir pressure along the crack. Current design codes provide the rules for these analyses and a comparison of criteria of three American regulatory agencies may be found in Ebeling et al. (2000), while the practice in various countries is discussed in Ruggeri (2004)

Finally, the historical information presented above is summarized in Figure 6, which systematizes the important scientific contributions and co-relates them with the main dams built.

## 3. Analysis of the stability of the historical profiles of Sazilly, Delocre and Rankine

A method of limit analysis was adopted for gravity dams based on the calculation of the static resultant, from the free body diagram of the dam, across various horizontal planes, which are

assumed to be potential failure planes. The failure scenarios analyzed for each plane are the sliding and the overturning[17]. The possibility of formation and evolution of a crack at the base is also evaluated, according to no-tension principle. The numerical application developed is presented in detail in Annex A.

For each cross-section geometry, the results presented below were obtained assuming a density of masonry and water of $\gamma^{mat} = 20kN/m^3$ and $\gamma^{ag} = 10kN/m^3$, respectively, and considering both horizontal and vertical components of hydrostatic pressure. The reservoir water level coincides with the maximum height of the dam, except in the analysis of the Delocre profile for which a reservoir water level of 50m was adopted. A downstream water level equal to zero and the absence of drainage system were considered, leading to a triangular uplift diagram for all cases. The sliding safety factors were calculated assuming a friction angle of 45º. The results obtained are:

– Thrust lines corresponding to the action of self weight and to the action of self weight plus hydrostatic pressure;

– Stress diagram and safety factors regarding failure at the base of the dam, given by the global analysis;

– Safety factors for horizontal planes within the body of the dam;

– Parametric analysis of the effect of the volumetric weight and of the friction angle on failure, at the base of the dam;

– Crack evolution at the base of the dam.

***Profile proposed by Sazilly in 1853***

Figure 7 presents the thrust lines due to the action of self weight (SW) and to the action of self weight and hydrostatic pressure (SW+HP), which are in agreement with the original

[17] Actually, the overturning does not occur in an isolated way, because once the process begins, it leads to the crushing of material close to the downstream toe of the dam, accompanied by sliding of the structure along that plane (Leclerc, Léger, and Tinawi 2003).

calculation of the author. The thrust line for the case of self weight and hydrostatic pressure presents small discontinuity points due to the application of the vertical component of hydrostatic pressure on the horizontal planes of the steps forming the upstream face.

Table 1 includes the total and effective vertical stresses at the base, due to the action of self weight and to the action of self weight plus hydrostatic pressure. It is observed that they comply with the limit of -6kgf/cm² (-0.59MPa), which is the criterion that served for the definition of the section. As a result of the uplift, a tensile stress, corresponding to +0.10MPa, is installed close to the upstream heel of the dam. Table 2 presents the safety factors for sliding and overturning, with and without uplift, for the action of self weight with hydrostatic pressure. It may be observed that, as a result of the uplift, the safety criterion (SF>1) is not met for the sliding scenario (SSF=0.94).

The sliding safety factors were also analyzed (Figure 8) for horizontal planes along the height of the dam. It may be concluded that the less favorable plane is not at the base, but rather is the plane coinciding with the end of the vertical section of the upstream face, 23m above the base (SSF=0.65). Figure 9 presents the sliding safety factors, which were obtained by the parametric analysis of volumetric weight of the dam, for a friction angle of 45º. The safety criterion is only achieved (SF>1), as regards the sliding scenario, for a volumetric weight higher than 20.75kN/m³. A similar analysis was done for the friction angle (Figure 10), for a volumetric weight of 20kN/m³. In this case, the safety scenario is only achieved (SF>1) for a friction angle higher than 46.75º.

As previously mentioned, the uplift pressure causes a tensile stress close to the upstream heel of the dam, being responsible for the formation of an initial crack depth of 7.9m at that location. Assuming a no-tension criteria, a new equilibrium state was established, with an extended crack length of 11.3m long, i.e., 22% of the base (Table 3). If full uplift is installed on that cracked section, the profile is not stable.

***Profile proposed by Delocre in 1866***

Figure 11 presents the thrust lines referring to the action of self weight (SW) and to the action of self weight with hydrostatic pressure (SW+HP) which are in agreement with the original calculation of the author. The thrust line for self weight with hydrostatic pressure also presents discontinuity points, close to the base, due to the application of the vertical component of hydrostatic pressure on the horizontal planes of the steps forming the upstream face in that zone. Table 1 shows the total and effective vertical stresses at the base for the two load scenarios, SW and SW+HP. For the case SW+HP, the calculated stresses are a little higher than the limit stress defined in the original project (-0.59MPa), presenting the value of -0.66MPa at the upstream heel of the dam. Due to uplift, a tensile stress is installed, corresponding to +0.09MPa, close to the upstream heel. Table 2 presents the sliding and overturning safety factors, with and without uplift, for the two load cases. Due to uplift, the sliding safety factor is slightly lower than 1 (SSF=0.99).

The analysis of safety factors within the body of the dam was made (Figure 8) and indicates that the less favorable plane corresponds to the base of the dam. Figure 9 presents the sliding safety factors, which were obtained by the parametric analysis of the volumetric weight of the dam, for a friction angle of 45º. The sliding safety criterion is only achieved (SF>1) for a volumetric weight higher than 20.25kN/m³. A similar analysis was done for the friction angle (Figure 10), for a volumetric weight of 20kN/m³. In the latter case, the safety scenario is only met (SF>1) for a friction angle higher than 45.25º.

As regards cracking, and similarly to the Sazilly's profile, the initial crack depth is 6.7m, while the final one extends to 9.2m (19% of the cracked base) (Table 3).

***Profile proposed by Rankine in1872***

Figure 12 shows the thrust lines produced by the action of self weight (SW) and the action of the self weight with hydrostatic pressure (SW+HP). For the thrust line due to the action of self

weight, there is an agreement with the original calculation of the author, whereas the thrust line for self weight with hydrostatic pressure differs from the original one because Rankine disregarded the vertical component of the hydrostatic pressure.

The total and effective vertical stresses at the base were computed (Table 1), for both load cases, SW and SW+HP. It may be observed that these comply with the limits of -9.8kgf/cm² (-0.96MPa), for upstream, and of -7.6 kgf/cm² (-0.75MPa), for downstream, which were defined in the original work. However, a tensile zone is detected, for self weight only, close to the downstream toe, with a value of +0.06MPa and, similarly to the other analyzed profiles, a tensile zone is also installed, due to uplift, with a value of +0.08MPa, close to the upstream heel. Table 2 presents the sliding and overturning safety factors, with and without uplift, for the action of self weight with hydrostatic pressure. It is observed that, due to the uplift, the safety criterion (SF>1) is not reached for the sliding scenario (SSF=0.67). This factor is worsened by Rankine's option of increasing the base of the dam, with a view to decrease the stress on the upstream face, thus enlarging the surface subject to uplift action.

The analysis of the sliding safety factors (Figure 8) throughout the body of the dam leads to the conclusion that the less favorable plane corresponds to the base of the dam. Figure 9 presents the sliding safety factors, obtained by the parametric analysis of the volumetric weight of the dam, for a friction angle of 45º. The safety criterion is only achieved (SF>1) for a volumetric weight higher than 24.25/m³. A similar analysis was done with respect to the friction angle (Figure 10), for a volumetric weight of 20kN/m³. In this case, the safety criterion is only achieved (SF>1) for a friction angle higher than 56.25º.

The section presents an initial crack depth at the base of 8.2m and a final crack of 11.8m (22% of the cracked area) (Table 3).

## 4. Discussion

The contributions of Sazilly, Delocre, Rankine and of other 19th century engineers allowed the design of gravity dams to be rooted on a scientific basis. This approach followed the developments in the discipline of Strength of Materials, after a long period of empirical practices. The three profiles that have been analyzed in this paper reflect the main concern at that time, which was to avoid compressive failure of masonry. The role of pore-pressure was neglected until the accident of Bouzey dam brought attention to its relevance, leading to the work of Lévy and others. Drainage was recognized as essential for the safety of gravity dams and was contemplated in new dam designs. The excessive length of the dam base, as proposed in the 19th century, increases the uplift force on the dam and reduces the safety factor with respect to sliding, which is usually the most critical failure mode in gravity dams. This failure scenario may involve sub-horizontal rock joints at shallow depth or the dam-foundation interface (e.g. Rocha 1978), as well as joints in the masonry body or lift joints in concrete dams (e.g. Léger et al. 1997). The assessment of safety with respect to sliding may be performed by straightforward static calculations, such as the application presented in this paper. The uplift pressure diagrams presently employed, and prescribed in design codes, were devised after monitoring data of water pressures in dam foundation became available, mainly with the dam construction programs of the 1930s and 1940s, as reported in Casagrande's influential Rankine lecture of 1961. Performing the same type of analysis for a standard modern gravity dam with a height to base ratio of 1:0.8, assuming the same properties, leads to sliding safety factors of 1.62 without uplift pressure and 0.83 with the triangular uplift diagram. Therefore the consideration of full uplift diagram, resulting from the absence or ineffectiveness of drainage, is a very penalizing scenario. Traditional construction practice always stressed the importance of achieving a good contact along the foundation surface, relying on rough, stepped or inclined profiles to provide the friction required to keep many of these old structures in safe operation. It should be noted that, after centuries of successful use,

the gravity dam remains a competitive option for new dams, nowadays mainly through the new roller-compacted concrete technology.

Safety assessment and rehabilitation of old masonry dams is presently under way in several countries. The understanding of the original design assumptions is essential for a correct intervention. Often, internal water pressures and foundation uplift pressures are the key issue. Improvement of drainage is usually required, either in the dam body, the foundation rock mass or in both. Various options are also available to reduce the permeability of masonry and the foundation rock, or to make the upstream dam face impervious (e.g. Bettzieche, Deutch, and Heitfuss 2004; Royet et al. 1993; Wittke, Schröder, and Polczyk 2003; Sagrado and Hernández 2001; Hortelano 2004).

## 5. Concluding remarks

A study has been presented of three historical profiles proposed for masonry dams in the 19th century, which had a profound effect on the evolution of dam design. These profiles were based mostly on a compressive strength criterion, since the role of uplift pressures and the importance of failure mechanisms involving sliding on horizontal planes were only fully recognized at a later date, leading to changes in design geometry and the implementation of drainage systems. Rehabilitation of these old structures, many still in use, requires a good understanding of the original assumptions. The analysis of the historical profiles was carried out with an application based on limit equilibrium concepts, which is capable of assessing the more common failure modes, and provides a very helpful tool for rehabilitation studies.

**Acknowledgements**

This work has been funded by FCT (Portuguese Foundation for Science and Technology) through the PhD grant SFRH/BD/43585/2008, for which the first author is grateful.

## Annex A – Numerical application for global stability analysis of gravity dam profiles

*Initial assumptions*

The loads involved in the limit analysis (Figure 13) are as follows: self weight $W$; upstream horizontal hydrostatic pressure ($HP_{h,u}$); upstream vertical hydrostatic pressure ($HP_{v,u}$); downstream horizontal hydrostatic pressure ($HP_{h,d}$); downstream vertical hydrostatic pressure ($HP_{v,d}$); upstream horizontal hydrodynamic pressure ($HdP_{h,u}$); upstream vertical hydrodynamic pressure ($HdP_{v,u}$); inertial force of the body of the dam ($I_h$); resultant of the uplift at the base between the upstream face and the drainage gallery ($U_{tot,u-g}$); and resultant of the uplift between the gallery and the downstream face ($U_{tot,g-d}$).

A plane analysis is considered in the model, meaning that it must be applied to straight gravity dams built on wide valleys. For dams presenting a small curvature in plan[18], the resistant portion due to the arch effect is disregarded and, hence, the results are somewhat conservative. The use of three-dimensional models is recommended for a more accurate estimate. For gravity dams built on narrow valleys, 3D analysis may also be advisable. In this case, the height of blocks can significantly vary, and there is the possibility of occurrence of a relevant global effect, dependent on the existence and effectiveness of shear keys in the vertical joints, which can only be evaluated through 3D models (Lombardi 2007).

Furthermore, the method does not take into account the relative stiffness of the dam and foundation. If the foundation is highly deformable, or if it presents a high heterogeneity, the deformation cannot be disregarded since it influences the stresses developed on the body of the dam (Rocha 1978).

[18] Such reasoning is also applicable to straight gravity dams, because an arch effect is assumed to be established inside the dam thickness (Herzog 1989).

The compressive stresses installed on a gravity dam are usually fairly low, below the material strength, both for concrete[19] and for masonry, and the same can be stated for medium strength foundations, which is why, in a expedite calculation, compressive failure is not considered. On the other hand, the tensile strength is considered as null, which is an important aspect for the determination of the length of cracks occurring at the base, as well as for the application of the uplift, by the iterative procedure.

A Mohr-Coulomb failure model, with null cohesion, was adopted for the horizontal plane. Therefore, the friction angle is the only strength parameter considered. This is justified by the fact that cohesion is difficult to determine by experimental means and has a high variability. Hence, most international regulations require the use of a high partial safety factors, or disregard it completely. On the other hand, cohesion only acts in practice when the section is under a minimum compressive stress, so if this aspect is not observed, it would be unsafe to consider it throughout the entire length of the plane under analysis (Leclerc, Léger, and Tinawi 2003).

Uplift is not considered as an external load, which is why it is not included in the free body diagram. Uplift is locally added to the total vertical stress to obtain effective stresses. If the foundation has a drainage system, it is assumed that the latter reduces the uplift, leading to a bi-linear uplift diagram, depending on the location of the gallery.

A seismic analysis method, designated as pseudo-static, is adopted, and it considers the inertial force of the dam and the hydrodynamic effect of water in accordance with Westergaard's solution. It is a simplified method that does not consider the amplification of the value of earthquake acceleration in height or its oscillatory characteristic, because the resultants are applied as static loads (Priscu et al. 1985).

*Data model*

[19] This is why the concrete dams use low strength or pozzolanic cement, with economical and practical reasons, because these cements have hydration temperatures lower than high strength cement.

The calculations are done on a model of data developed from the idealization of a discrete medium consisting of horizontal elements (Figure 14), which are geometrically represented by the corresponding axes, and defined by the intersections between planes, with upstream and downstream faces. The element thickness ($e$) may be chosen depending on the dam height. For instance, from several experiences done, values of $e = 0.10m$ have been adopted for dams with up to 30m height and of $e = 0.50m$ for the other cases.

The structure of the data consists of the following five parameters: length of the element ($L^n$), abscissa of the centre of the element ($x_c^n$), level of the axis of the element ($y^n$), abscissa close to the upstream face ($x_u^n$) and abscissa close to the downstream face ($x_d^n$). Only three of these parameters are independent ($x_u^n$, $x_d^n$, $y^n$), the remaining ones were introduced with the objective of optimizing the calculations and are determined as follows:

– length of the element

$$L^n = x_d^n - x_u^n$$

– abscissa of the centre of the element

$$x_c^n = \frac{x_u^n + x_d^n}{2}$$

The loads presented in Figure 13 are considered, at the level of element $n$, as follows (Figure 15):

– Self weight

$$W^n = L^n e \gamma^{mat}$$

– Upstream horizontal hydrostatic pressure

$$HP_{h,u}^n = \left(z_{HP,u} - y^n\right)\gamma^{ag} e \Leftrightarrow z_{HP,u} \geq y^n$$

– Upstream vertical hydrostatic pressure

$$HP_{v,u}^n = \left(z_{HP,u} - y^n\right)\gamma^{ag}\left(x_u^n - x_u^{n+1}\right) \Leftrightarrow z_{HP,u} \geq y^n$$

– Downstream horizontal hydrostatic pressure

$$HP_{h,d}^{n} = \left( z_{HP,d} - y^{n} \right) \gamma^{ag} e \Leftrightarrow z_{HP,d} \geq y^{n}$$

– Downstream vertical hydrostatic pressure

$$HP_{v,d}^{n} = \left( z_{HP,d} - y^{n} \right) \gamma^{ag} \left( x_{d}^{n+1} - x_{d}^{n} \right) \Leftrightarrow z_{HP,d} \geq y^{n}$$

– Upstream horizontal hydrodynamic pressure[20]

$$HdP_{h,u}^{n} = \frac{7}{8} a_h \gamma^{ag} \sqrt{\left( z_{HP,u} - y_{found} \right) \left( z_{HP,u} - y^{n} \right)} e \Leftrightarrow z_{HP,u} \geq y^{n}$$

– Upstream vertical hydrodynamic pressure

$$HdP_{v,u}^{n} = \frac{7}{8} a_h \gamma^{ag} \sqrt{\left( z_{HP,u} - y_{found} \right) \left( z_{HP,u} - y^{n} \right)} \left( x_{u}^{n} - x_{u}^{n+1} \right) \Leftrightarrow z_{HP,u} \geq y^{n}$$

– Inertial load

$$I_{h}^{n} = L_n e \gamma^{mat} a_h$$

In which,

$\gamma^{mat}$ – Volumetric weight of the material

$\gamma^{ag}$ – Volumetric weight of water

$z_{HP,u}$ – Upstream water level

$z_{HP,d}$ – Downstream water level

$y_{found}$ – Foundation level

$a_h$ – Seismic coefficient, horizontal direction

It is observed that the hydrostatic and the hydrodynamic pressures acting on the face of an element present a rectangular distribution, which corresponds to an acceptable approximation for small thickness elements ($e$). For a given horizontal plane, the analysis is done from the integration of the elements ($e$) placed above such plane. In order to achieve the consistency

[20] Parabolic approximation proposed by Priscu (1985), for Westergaard's solution.

of the model, the smaller the discretization thickness, the higher the accuracy of results, i.e., by taking as example the self weight, it is possible to obtain convergence to the true solution:

$$\lim_{e\to 0}\left|\sum W^n - W\right| \to 0$$

*Determination of results*

The application makes possible to visualize the thrust lines due to the action of self weight, corresponding to the situation of empty reservoir, and to the action of self weight with other actions. The concept of thrust line results from the graphic statics and corresponds to the geometrical place occupied by the static resultant in each horizontal plane of loads applied above that plane (Henkel 1943). It has an important physical meaning, because it represents the load distribution across the body of the structure (Heyman 1995). Through its observation, it is possible to identify tensile zones, which is the case of the planes in which the thrust line is located outside the central third of the section. Furthermore, it is also possible to observe on a graph the diagram of total and effective vertical stresses. The total stresses are obtained in the following way:

$$\sigma = \frac{\sum V}{A} \pm \frac{\sum M}{I} y\,,$$

in which,

$\sigma$ – Upstream and downstream total vertical stress;

$\sum V$ – Sum of the vertical component of actions[21];

$\sum M$ – Sum of moments due to actions;

$A$ – Area of the base (per meter of the dam length);

$I$ – Inertial moment of the plane (per meter of the dam length);

$y$ – Distance to the downstream and upstream faces.

[21] Except for uplift, because, the latter was not considered as an external action.

The effective stresses are determined from total stresses by adding the uplift pressure. Generally, the uplift diagram presents a bi-linear configuration (Figure 16a), resulting from the triangular diagram and from the effect of the reduction in the drainage system. The diagram can be updated whenever a new crack arises, close to the upstream face, where the full uplift is applied (Figure 16b and Figure 16c), leading to the iterative calculation of the final length of the crack. The initial length of the crack, for a previously defined load scenario, is determined on the basis of the criterion of null tensile resistance. The calculation of the final length of the crack takes into account the assumptions as follows:

- after the occurrence of the initial crack, it may be considered that the drainage system loses totally (Figure 16b) or partly (Figure 16c) its effectiveness (e.g. Ebeling et al. 2000; Ruggeri 2004), and, therefore, the pressure diagram acquires a rectangular configuration along the crack and a trapezoidal or triangular configuration, depending on the downstream water level, along the non-cracked surface;

- unlike the previously adopted strategy, the uplift becomes part of the eccentricity and stress calculations; otherwise it would not be possible to establish an iterative calculation method to simulate the progression of the crack.

The factor of safety to sliding (SSF), in any horizontal plane, including the base, for the actions applied above their level, is given by:

$$SSF = \frac{\left(\sum V\right)\tan\phi}{\sum H},$$

in which,

$\sum V$ – Sum of the vertical component of actions[22];

$\tan\phi$ – Tangent of the friction angle;

$\sum H$ – Sum of the horizontal component of actions.

[22] Including the uplift. In this case, the effect of uplift can be physically interpreted as a factor of reduction in self weight (Serafim 1968)

The overturning safety factor (OSF) is given by:

$$OSF = \frac{\sum M_{sta}}{\sum M_{ope}},$$

in which,

$\sum M_{sta}$ – Sum of stabilizing moments;

$\sum M_{ope}$ – Sum of acting moments.

For the analysis throughout the body of the dam, in the various horizontal planes defined from the thickness ($e$), the full uplift is considered for these levels, without any reduction factor, because it is assumed that there is no vertical drainage system installed on the body of the dam. The other actions reflect the load cases adopted.

The available parametric analysis, for the self weight and the friction angle, refer to the horizontal plane of contact between the dam and the foundation and to the load cases considered, according to the hypotheses admitted for the uplift.

**References**

Almeida, F. 1969. Sobre a barragem romana de Olisipo e seu aqueduto. O Arqueólogo Português III:180-189.

Bettzieche, V., R. Deutch, and C. Heitfuss. 2004. 100 Years of Experience in Ageing of Masonry Dams and life-time-based Rehabilitation. Paper read at 2nd International Conference on Lifetime Oriented Design Concept - ICOLD 2004, at Bochun.

Billington, D.P., D.C. Jackson, and M.V. Melosi. 2005. The history of large federal dams: Planing, design and construction in the era of big dams. Denver: Bereau of Reclamation - U.S. Departament of the Interior.

Casagrande, A. 1961. First Rankine Lecture: Control of seepage through foundations and abutments of dams. Géotechnique - The International Journal of Soil Mechanics XI:161-182.

Chanson, H., and D.P. James. 2002. Historical Development of Arch Dams: from cut-stone arches to modern concrete designs. Australian Civil Enginnering Transactions CE43:39-51.

Clough, R.W., and E.L. Wilson. 1999. Early finite element research at Berkeley. In Fifth U.S. National Conference on Computational Mechanics.

Davidson, I. 1997. George Deacon (1843-1909) and the Vrynwy works. Vol. 4, Studies in the History of Civil Engineering: Dams.

Delocre, F. 1866. Mémoire sur la forme du profil à adopter pour les grands barrages en maçonnerie des réservoirs. *Annales des Ponts et Chassées*.Ebeling, R.M, L.K Nuss, F.T. Tracy, and B. Brand. 2000. Evaluation and Comparison of Stability Analysis and Uplift Criteria for Concrete Gavity Dams by Three Federal Agencies. Washington, DC: U.S.Army Corps of Engineers.

Hager, W.H., and C. Gisonni. 2007. Augsute Graeff: Dam designer and hidraulic engineer. Journal o Hydraulic Engineering - ASCE:241-247.

Henkel, O. 1943. Estática Gráfica. Barcelona: Editorial Labor.

Herzog, M.A.M. 1989. Spatial action of straight gravity dams in narrow valleys. Journal of Structural Engineering 115:698-706.

Heyman, J. 1995. The stone skeleton - Structural engineering of masonry architecture. Cambridge: University of Cambridge.

Hortelano, A.M. 2004. Presas de mampostería. Madrid: Ministerio de Fomento.

Jackson, D.C. 1997. Studies in the History of Civil Engineering: Dams. Vol. 4.

Jansen, R.B. 1980. Dams and Public Safety. Denver: Departamento of the Interior - Bereau of Reclamation.

Laá, G.G. 1993. Masonry dams inspection. Paper read at Technical symposium on maintenance of older dams, at Chambery.

Leclerc, M., P. Léger, and R. Tinawi. 2003. Computer aided stability analysis of gravity dams - CADAM. Advances in Engineering Software:403-420.

Lombardi, G. 2007. 3-D analysis of gravity dams. Hydropower & Dams (One):98-102.

Londe, P. 1987. The Malpasset Dam failure. Paper read at Workshop on Dam Failures - Engineering Geology, at Purdue.

Léger, P., R. Tinawi, S.S. Bhattacharjee, and M. Leclerc. 1997. Failure mechanisms of gravity dams subjected to hydrostatic overload: influence of weak lift joints. Paper read at XIX Congress on Large Dams, at Florence.

Lévy, M.M. 1895. Quelques considérations sur la construction de grands barrages. Comptes-Rendus de l'Académie des Sciences 6:288-300.

Parra, M.A., J.I.H. Domínguez, F.J. Dillet, C.D.G. Jaén, and R.C. Gimeno. 1995. La presa romana de Almonacid de La Cuba y otros aprovechamientos antiguos en el Río Aguasvivas. *Revista de Obras Públicas* 3345:43-66.

Priscu, R., A. Popovici, D. Stematiu, and C. Stere. 1985. Earthquake Engineering for Large Dams. 2 ed. Bucarest: John Wiley & Sons.

Quintela, A.C., J.L. Cardoso, and J.M Mascarenhas. 1987. Roman dams in southern Portugal. Water Power & Dam Construction:38-40,70.

Rankine, W.J.M. 1881. Miscellaneous scientific papers: Report on the design and construction of masonry dams. London: Charles Griffin and Company.

Rissler, P. 1993. The Intze-type masonry dams in Germany: recent safety assessments, adaptations and repairs. Paper read at Technical symposium on maintenance of older dams, at Chambery.

Rocha, M. 1978. Analysis and design of the foundations of concrete dams. In Intertional Symposium on Rock Mechanics Applied to Dam Foundations. Rio de Janeiro.

Royet, P., J. Franq, L. Bayet, and J.M Boutet. 1993. Diagnosis and rehabilitation of masonry dams. Paper read at Maintenance of older dams, at Chambery.

Ruggeri, G. 2004. Uplift Pressures under Concrete Dams. ICOLD European Group.

Sagrado, J.D., and F.B. Hernández. 2001. Ingeniería de presas: presas de fábrica: Universidad de Cantabria.

Sazilly, J.A.T. 1853. Note sur un type de profil d'égale résistance proposé pour les murs de réservoirs d'eau. Annales des Ponts et Chassées 6:191-222.

Schnitter, N.J. 1994. A history of Dams – The useful pyramids. Rotterdam: A.A. Rotterdam.

Serafim, J.S. 1968. Influence of Interstitial Water on the Behavior of Rock Masses. In Rock Mechanics in Engineering Practice, edited by K. G. Stagg and O. C. Zienkiewicz. London: John Wiley & Sons.

Smith, N. 1971. A history of dams. London: Peter Davies.

Vogel, A. 1981. The History of Large Dams. Osterreichische Wasserwirtschaft 33.

Wegmann, E. 1899. The desing and construction of dams. New York: John Wiley & Sons.

Westergaard, H.M. 1933. Water pressure on dams during earthquakes. *Transactions of ASCE* 98:418-433.Wittke, W., D. Schröder, and H. Polczyk. 2003. Upgrading the stability of three masonry dams in different ways. In *ISRM 2003–Technology roadmap for rock mechanics*, edited by S. A. I. o. M. a. Metallurgy.

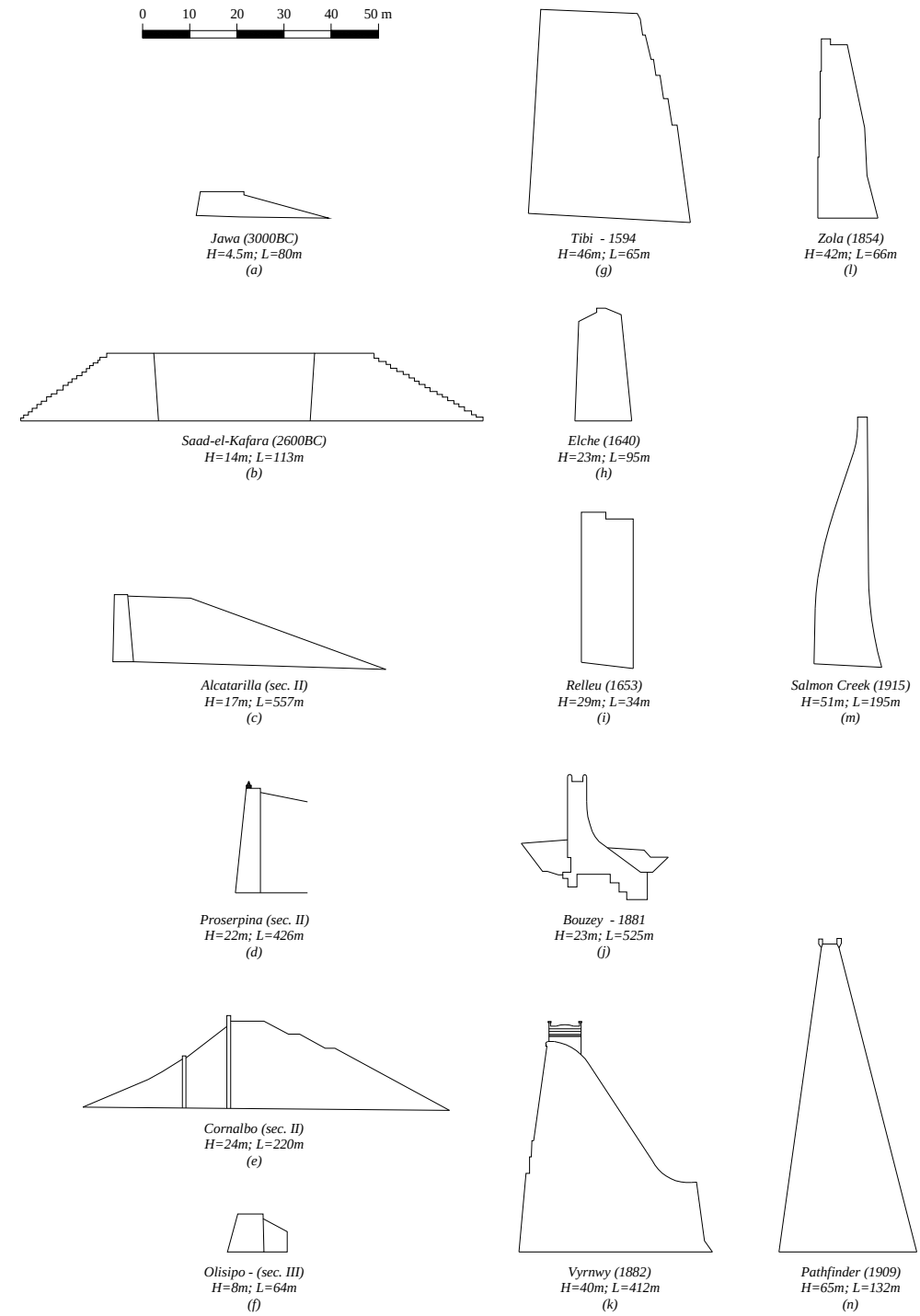


Figure 1 – Profiles of historical dams

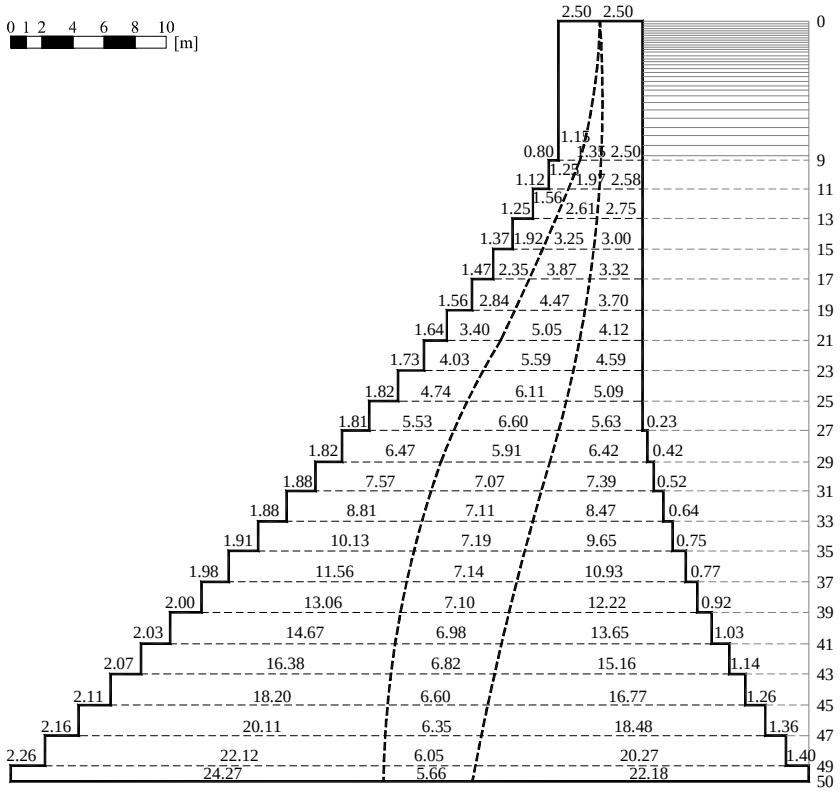


Figure 2 – Profile proposed by Sazilly

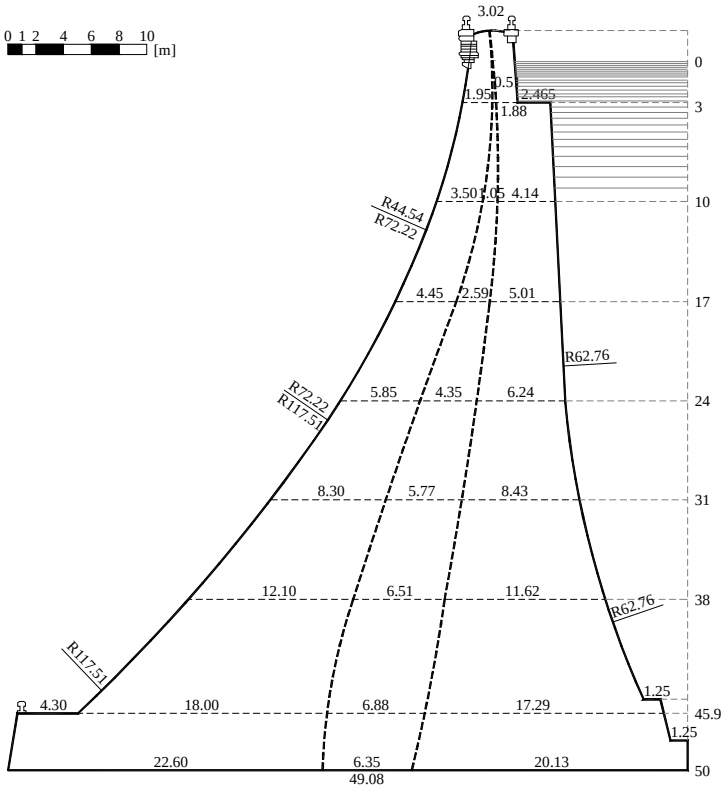


Figure 3 – Cross-section of Furens Dam designed by Delocre

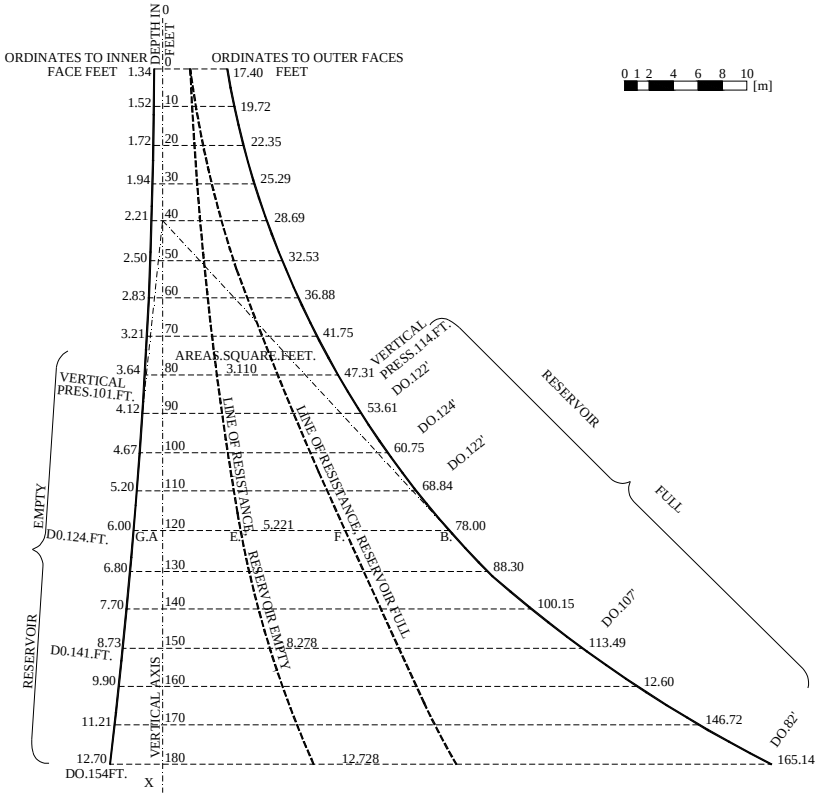


Figure 4 – Profile proposed by Rankine

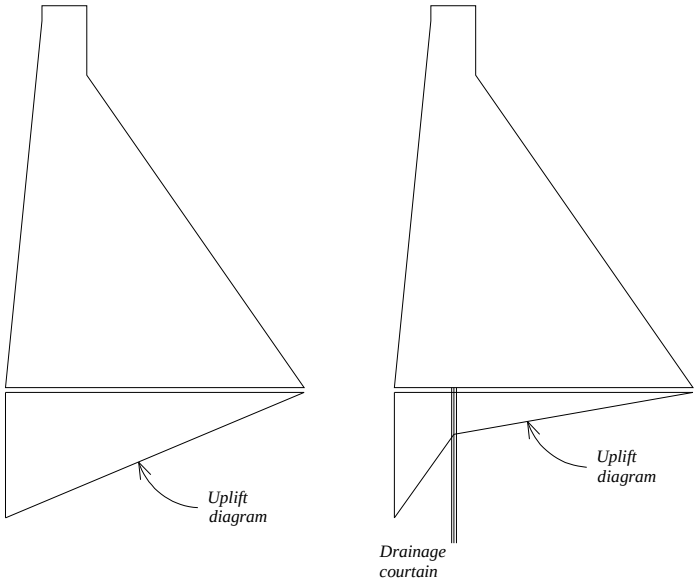


Figure 5 – Standard uplift diagram without drainage system (a) and with drainage system (b)

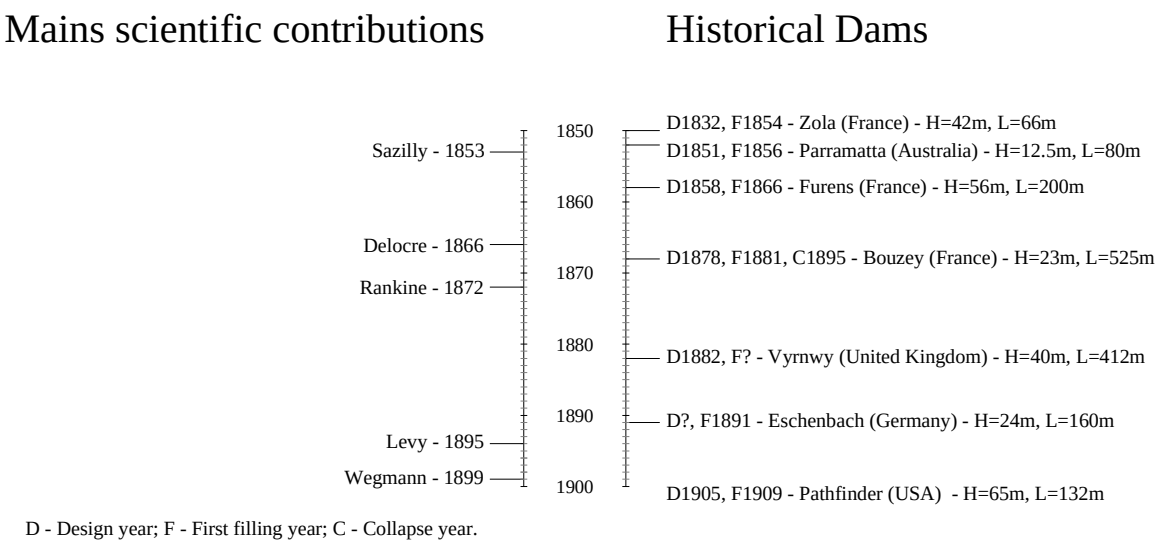


Figure 6 – Main contributions in the development of gravity dams during 19th century

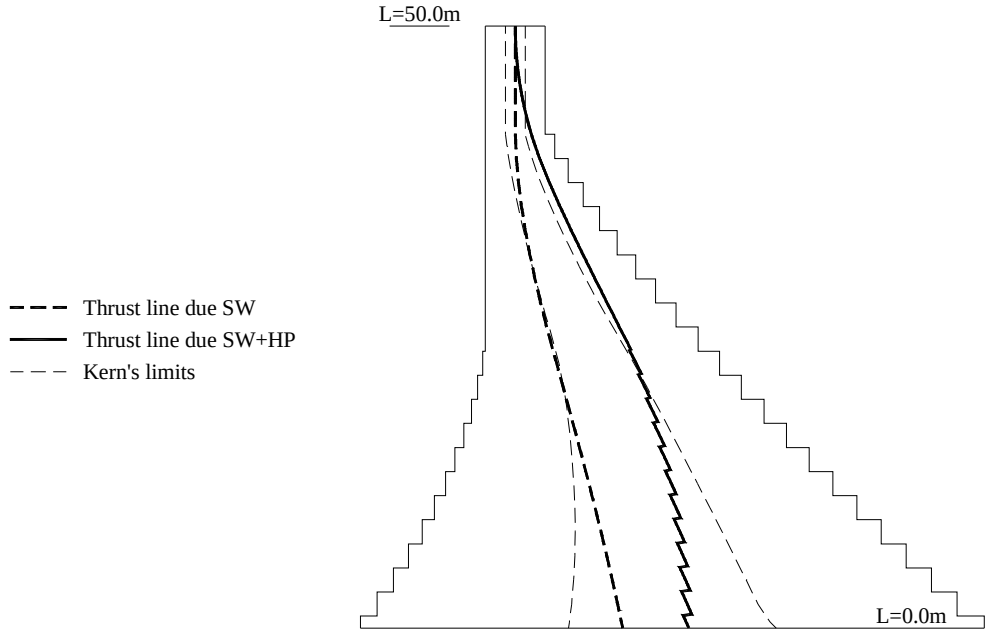


Figure 7 – Profile proposed by Sazilly: Thrust line due to self weight (SW) and self weight plus hydrostatic pressure (SW+HP)

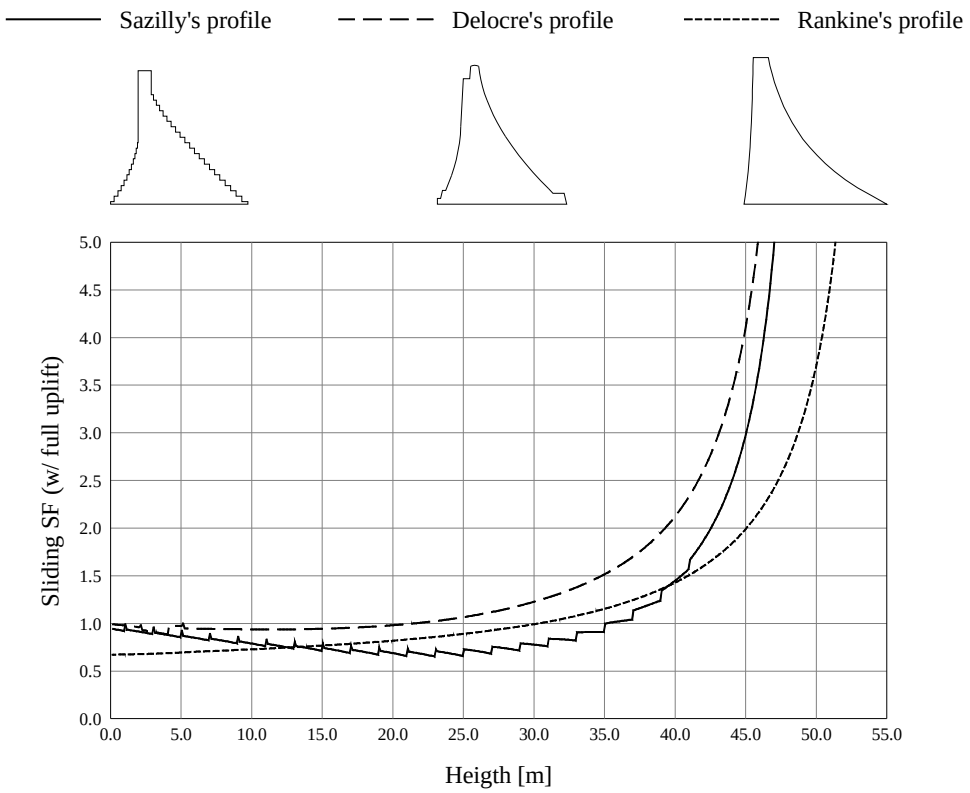


Figure 8 – Profiles proposed by Sazilly, Delocre and Rankine: Sliding safety factors for horizontal planes trough the dam height (self weight: 20kN/m³, friction angle: 45º and full uplift condition)

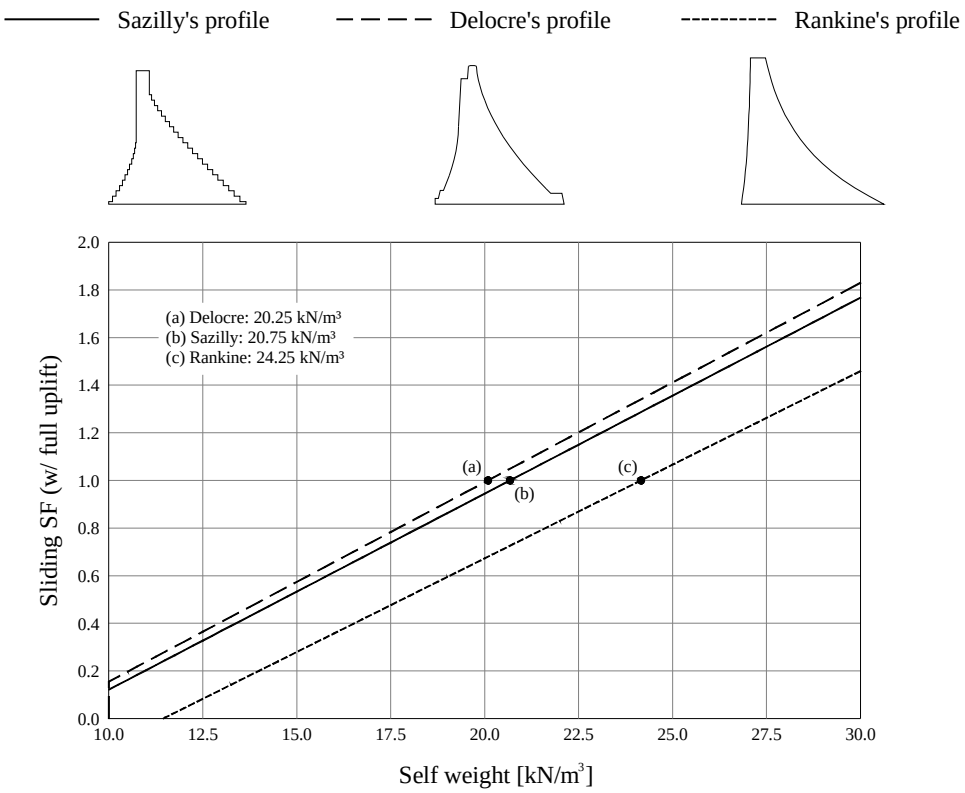


Figure 9 – Profiles proposed by Sazilly, Delocre and Rankine: Sliding safety factors for the dam base for a self weight parametric analysis (friction angle: 45º and full uplift condition)

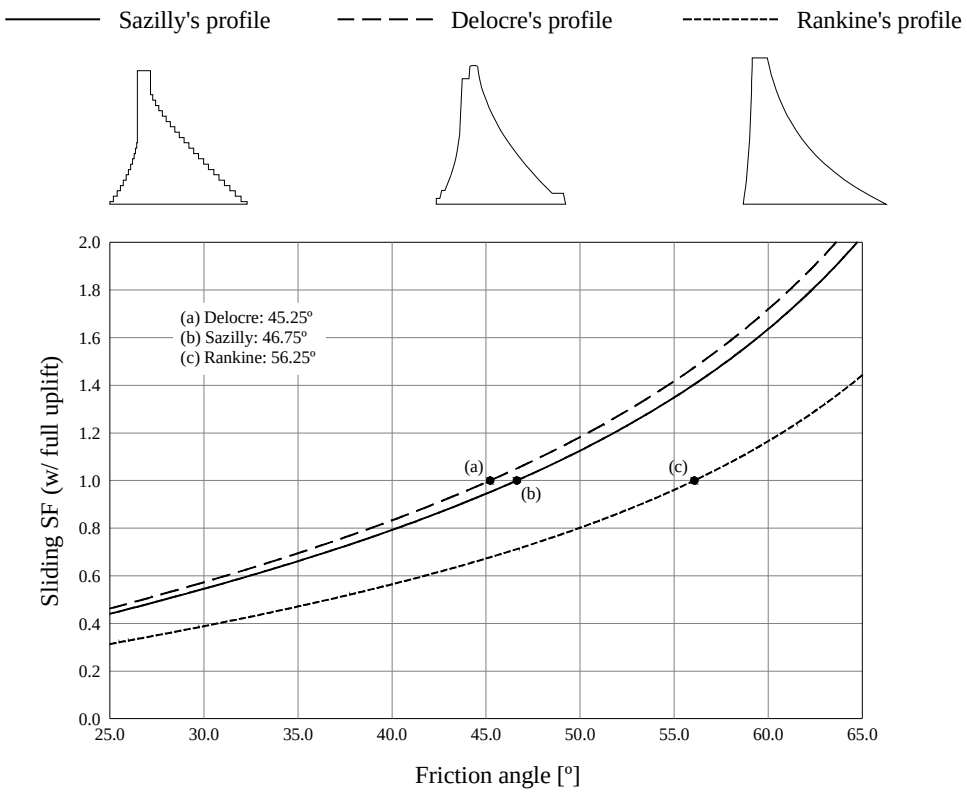


Figure 10 – Profiles proposed by Sazilly, Delocre and Rankine: Sliding safety factors for the dam base for a friction angle parametric analysis (self weight: 20kN/m³ and full uplift condition)

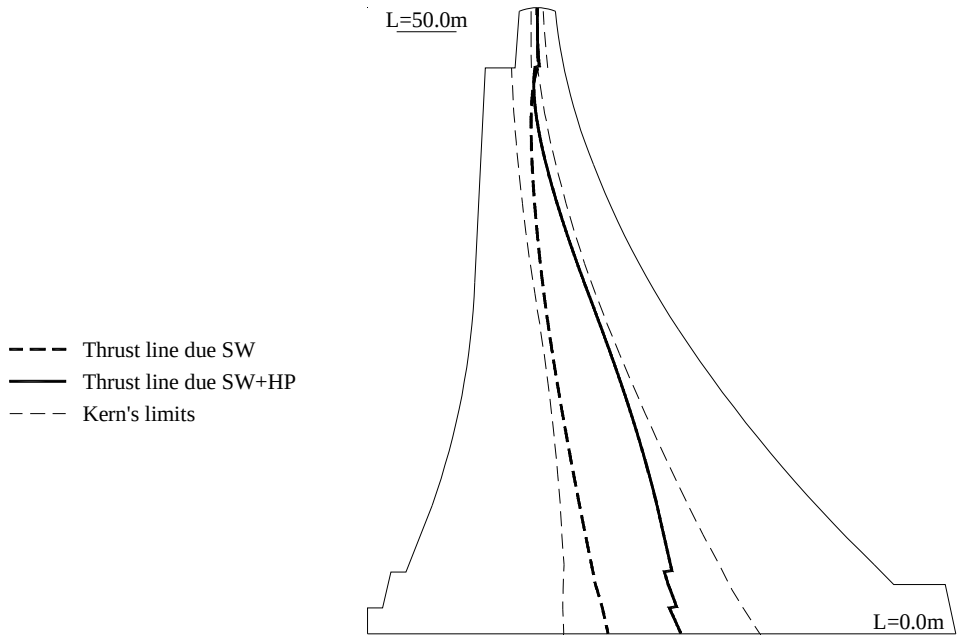


Figure 11 – Profile of Furens Dam designed by Delocre: Thrust line due self weight (SW) and self weight plus hydrostatic pressure (SW+HP)

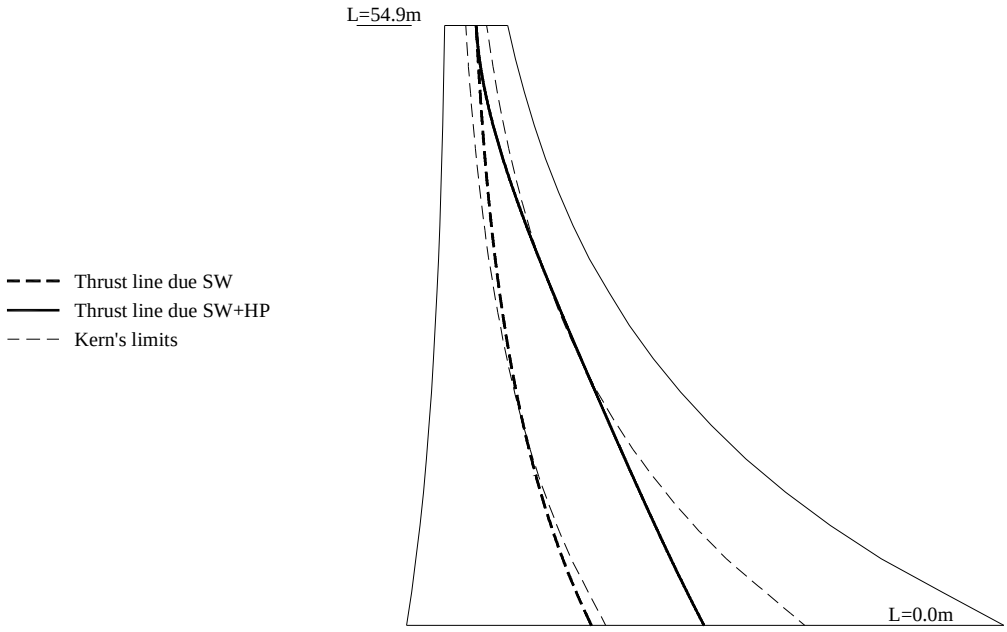


Figure 12 – Profile proposed by Rankine: Thrust line due self weight (SW) and self weight plus hydrostatic pressure (SW+HP)

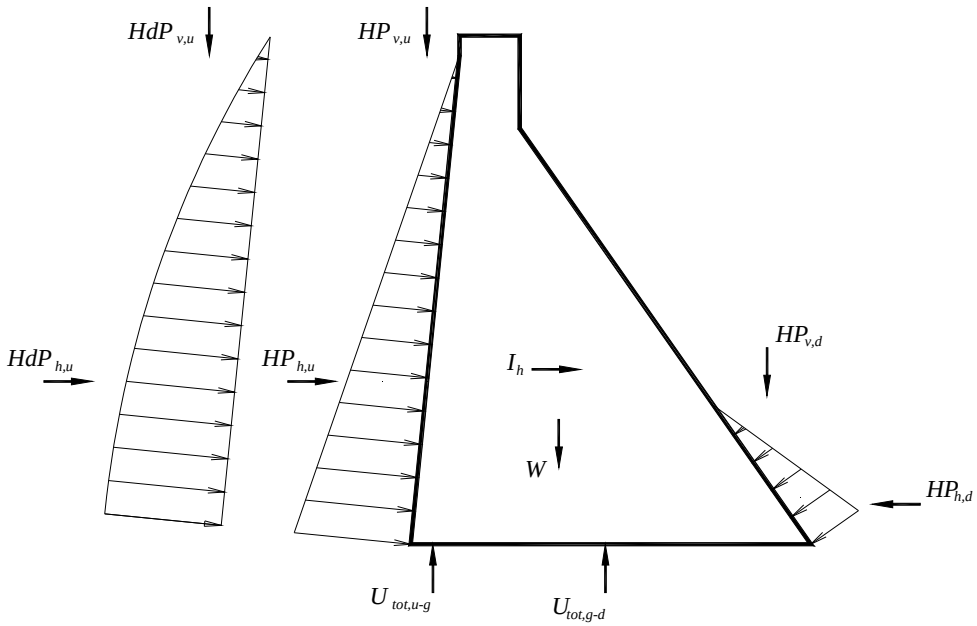


Figure 13 –Loads considered in the numerical tool

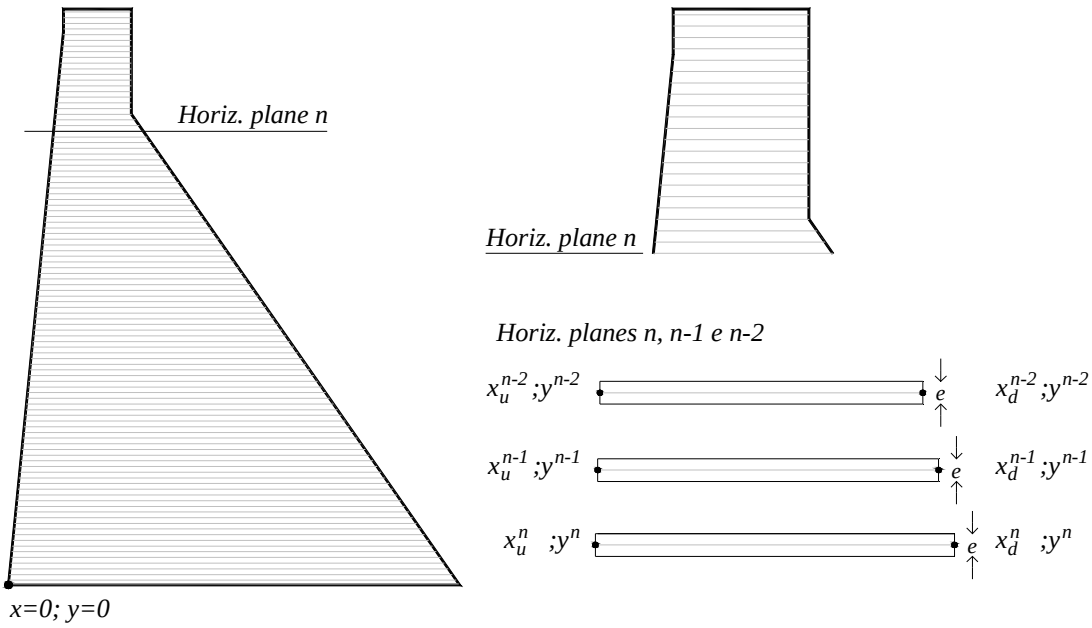


Figure 14 – Discretization scheme of the dam body

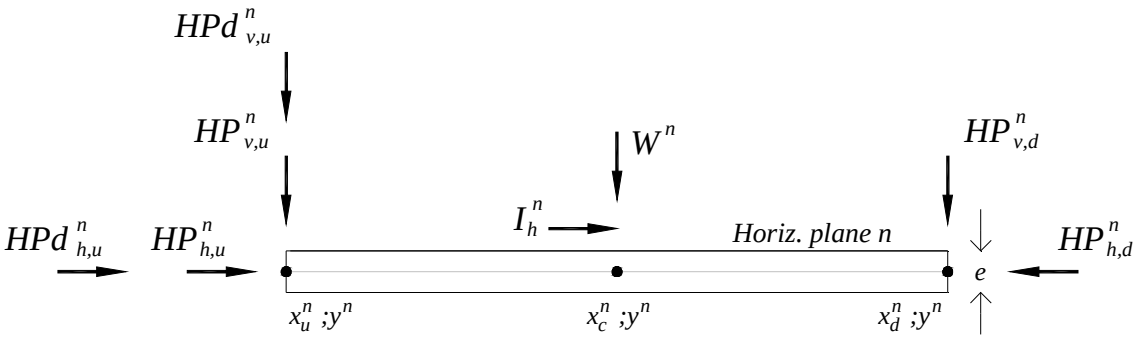


Figure 15 – Load representation in single element

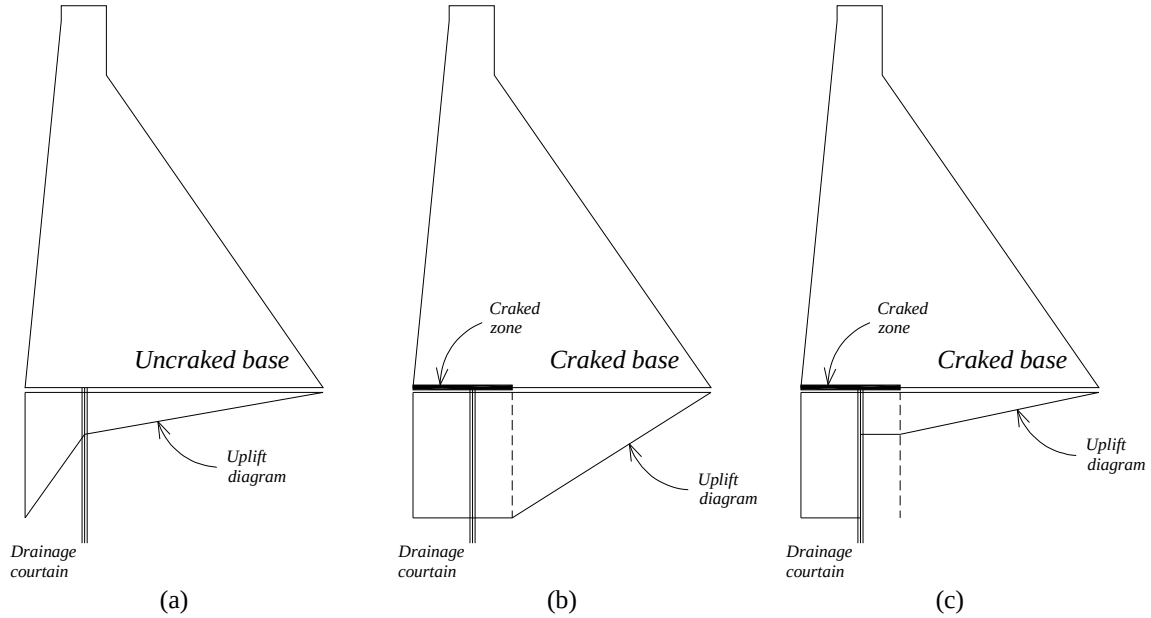


Figure 16 – Uplift diagram for uncracked base (a), cracked base with totally damage drainage system (b) and cracked base with partial damage drainage system (c)

Table 1 – Profiles proposed by Sazilly, Delocre and Rankine: Total and effective vertical stresses at the base due self weight (SW) and self weight with hydrostatic pressure (SW+HP) [MPa]

| | Sazilly's profile | | Delocre's profile | | Rankine's profile | |
|---|---|---|---|---|---|---|
| | Heel | Toe | Heel | Toe | Heel | Toe |
| SW (Total stress) | -0.58 | -0.21 | -0.66 | -0.19 | -0.94 | +0.06 |
| SW+HP (Total stress) | -0.40 | -0.55 | -0.41 | -0.60 | -0.47 | -0.46 |
| SW+HP (Effective stress) | +0.10 | -0.55 | +0.09 | -0.60 | +0.08 | -0.46 |

Table 2 – Profiles proposed by Sazilly, Delocre and Rankine: Sliding (SSF) and overturning safety factors (OSF) due to the combination of self weight and hydrostatic pressure [-]

| | Sazilly's profile | | Delocre's profile | | Rankine's profile | |
|---|---|---|---|---|---|---|
| | w/o uplift | w/ uplift | w/o uplift | w/ uplift | w/o uplift | w/ uplift |
| OSF | 3.95 | 1.24 | 3.73 | 1.27 | 3.47 | 1.18 |
| SSF | 1.99 | 0.94 | 1.97 | 0.99 | 1.66 | 0.67 |

Table 3 – Profiles proposed by Sazilly, Delocre and Rankine: Cracking propagation and final sliding safety factors (SSF) due self weight with hydrostatic pressure

| | Initial SSF | Initial crack length [m] | Final crack length [m] | Final cracked base percentage |
|---|---|---|---|---|
| Sazilly's profile | 0.94 | 7.9 | 11.3 | 22% |
| Delocre's profile | 0.99 | 6.7 | 9.2 | 19% |
| Rankine's profile | 0.67 | 8.2 | 11.8 | 22% |